ACS APPLIED MATERIALS & INTERFACES

Research Article

www.acsami.org

Electrochemical Method Assisted Immobilization and Orientation of Myoglobin into Biomimetic Brij 56 Film and Its Direct Electrochemistry Study

Qin Xu,*[,†,‡] Yuanyuan Shen,[†] Jiaqian Tang,[†] Min-Hua Xue,[‡] Liping Jiang,[‡] and XiaoYa Hu*[,†]

[†]College of Chemistry and Chemical Engineering, Yangzhou University, Yangzhou 225002, China

[‡]College of Chemistry and Chemical Engineering, Nanjing University, Nanjing 21009, China

ABSTRACT: A simple cyclic voltammetric method was applied to assemble and orient a model protein, namely, myoglobin (Mb), into a biocompatible Brij 56 film. Ultraviolet−visible and circular dichroism spectra indicated that Mb in Brij 56 matrix preserved its secondary structure. Fourier transform infrared spectra confirmed the formation of hydrogen bonds between Mb and Brij 56. These hydrogen bonds acted as the electron tunnel to transfer electrons from Mb's active sites to the underlying glassy carbon electrode. Effective direct electron transfer of Mb was realized with the presence of a couple of quasi-reversible and well-defined redox peaks at −310 mV (vs standard calomel electrode) in the studied potential range. The peaks were attributed to the redox couple of heme Fe(II)/Fe(III) of the well-oriented Mb in Brij 56 matrix. The surface coverage and the electron transfer rate (k_s) of Mb immobilized into the Brij 56 film was ~4.9×10^{-11} mol cm^{-2} and 72.6 ± 3.0 s^{-1}, respectively. An excellent electrocatalytic response of the immobilized Mb toward nitrite in the absence of electron transfer mediators was observed. These results emphasized that the biomimetic Brij 56 could be used as an attractive material for immobilizing proteins and constructing biosensors.

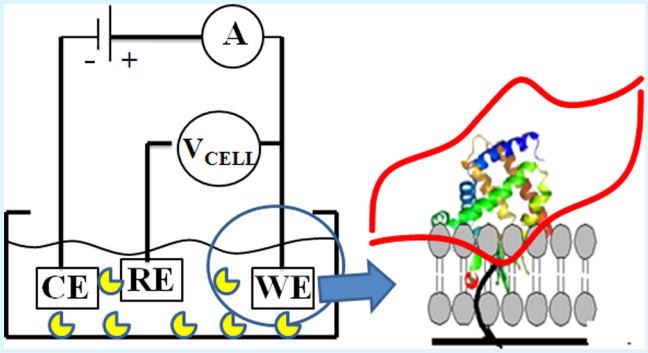

KEYWORDS: *myoglobin, Brij 56, cyclic voltammetric, orientation, direct electron transfer*

1. INTRODUCTION

Over the last years, many researches have been done to study the direct electrochemistry of redox proteins for the development of "third generation" biosensors,[1,2] environmentally sound biofuel cells,[3,4] heterogeneous catalysts,[5] and even biomolecular electronic components.[6−8] However, it is hard to obtain direct electron transfer (DET) between redox proteins and unmodified electrodes because the redox-active centers of proteins are buried in the polypeptide chains, and the biological protein matrix is instable when interacting with electrode surfaces.[9]

For realizing DET of proteins, choosing a suitable biocompatible matrix and performing the favorable active site orientation of proteins during the immobilization process are necessary.[10,11] Surfactants with amphiprotic structure can form supermolecule aggregates and have the gel-to-liquid crystal phase transitions characters, a phenomenon shared with biomembranes,[12] so they could present a friendly matrix for proteins immobilization to realize their DET.[13−15] DET of proteins in different kinds of surfactants has been reported. In most cases, ionic surfactants were used.[16−18] However, early studies showed that ionic surfactants would destroy protein structure and pull heme into solution.[19] Neutral surfactants have been reported to stabilize a couple of membrane protein[20] without influencing their structures. They should be better candidates for the immobilization of proteins.[21,22]

Polyethylene glycol hexadecyl ether (Brij 56), $C_{16}H_{33}(OCH_2CH_2)_nOH$, n = 10, is a kind of nonionic surfactant. It has been widely used to prepare mesoporous nanomaterials[23] because of its inexpensive, nontoxic, biodegradable, and structure-directing characters.[24,25] However, the study about the effect of Brij 56 on the activity of proteins and its application in the construction of biosensors is scant. Thus, one purpose of this work is to study the feasibility of Brij 56 for the immobilization of proteins.

In most cases, proteins and surfactants were modified on an electrode by a two-step procedure in which proteins were mixed with surfactants. Then the electrode surface was covered by the mixture and dried for use. However, it was hard to control the amount and orientation of proteins on electrodes by this method. Layer-by-layer (LbL) method may be an alternative.[26] Films obtained by LbL are well-ordered. Nevertheless, they are time-consuming,[27] and the catalytic activity of the immobilized proteins might be limited by substrate mass

Received: February 15, 2015
Accepted: May 8, 2015
Published: May 8, 2015

DOI: 10.1021/acsami.5b01492
ACS Appl. Mater. Interfaces 2015, 7, 11286−11293

transport when the numbers of protein layers was larger than two or three.[28] Considering these, the other aim of this work is to provide a new method to immobilize and orient proteins.

Herein, the cyclic voltammetric method was used to assist the assembly and orientation of proteins by using myoglobin (Mb) as a model into the biomimetic Brij 56 modified electrode. The DET characteristics and electrocatalytic behavior of the oriented immobilized Mb were thoroughly studied in this work.

2. EXPERIMENTAL SECTION

2.1. Chemicals and Materials. Brij 56 (98%) was purchased from Fluka. It was dissolved in pure water at 40 °C to achieve a concentration of 8 mg/mL. Myoglobin (Mb, MW 16 700, isoelectric point ≈ 6.9) was purchased from Sino-American Biotechnology Co. Ltd. in HeNan. All other chemicals were used directly. The deionized double-distilled water (18.6 MΩ·cm) (Millipore Co. Ltd.) was used to prepare all the solutions. NaH_2PO_4 and Na_2HPO_4 were mixed together to prepare phosphate buffer solutions, and the pH of the mixtures was adjusted by NaOH or H_3PO_4 solutions with the concentration of 1.0 M.

2.2. Apparatus and Methods. All the cyclic voltammetry and amperometry experiments were performed on a CHI 660a electrochemical analyzer (Shanghai Chenhua). An unmodified or modified glassy carbon electrode (GCE, 3 mm in diameter, Shanghai Chenhua) was used as the working electrode, a platinum foil acted as the counter electrode, and a saturated calomel electrode (SCE) was used as the reference electrode. Alumina slurries with the diameter size of 0.3 and 0.05 μm were used to polish the GCE to a mirrorlike surface before each experiment. Then, the polished GCE was sequentially rinsed with HNO_3 (1:1 v/v), ethanol (1:1 v/v), and doubly distilled water. All the ultraviolet−visible (UV−vis) absorption spectra were recorded on a UV-2510 spectrophotometer (Shimadzu, Japan). A Nicolet 400 Fourier transform infrared (FT-IR) spectrophotometer (Nocolet, USA) was used to obtain FT-IR spectra of Mb, Brij 56, and Mb/Brij 56. Circular dichroism (CD) measurements of Mb in the absence and presence of Brij 56 were achieved by a spectropolarimeter (JASCO J-810). Spectra were collected from 190 to 300 nm at the scan rate of 200 nm/min and a response time of 1 s. The average value of 10 scans was used to obtain each CD spectrum. All the atomic force microscopy (AFM) images were collected from an Agilent Technologies 5500 microscope (Santa Clara, CA) by using Olympus rectangular silicon nitride cantilevers at room temperature. The scanning rate was 1.411 lines per second. The picoimage software from Agilent was used to first-order flatten all images.

2.3. Electrode Modification Procedures. Two different procedures were used to prepare the Mb-Brij 56 film modified GCEs. In the first method, the freshly polished GCE was dipped into 8 mg/mL of Brij 56 solution at 35 °C for ∼1 h. The electrode was washed by distilled water after it was removed from Brij 56 solution and then was placed into 0.05 M phosphate buffer solution (pH 7.0) with 4 mg/mL Mb. Consecutive cyclic voltammograms (CVs) were performed on this Brij 56-modified electrode until steady-state CVs were obtained. This electrode was named Mb-Brij 56/GCE. An alternative was used by casting the mixture of Brij 56 and Mb on the electrode. For another electrode, 8 mg/mL Brij 56 (10 μL) and 8 mg/mL Mb (10 μL) were mixed together, and then a 5 μL aliquot of the mixture was spread on a freshly polished GCE. The electrode was then dried at room temperature and stored in a refrigerator overnight before it was used. This electrode was called Mb/Brij 56/GCE. Before using, the weakly adsorbed Mb on the two modified electrodes was washed gently by double-distilled water, and then the two kinds of electrodes were placed into 5 mL of 0.05 M phosphate buffer solution in the absence of Mb for all the electrochemical experiments. Prior to a series of experiments, oxygen in the phosphate buffer solutions was removed by purging with purified nitrogen for at least 10 min

3. RESULTS AND DISCUSSION

3.1. Characterization of the Interaction between Mb and Brij-56. UV−vis absorption spectroscopy was used to study protein−surfactant interactions. The UV−vis spectra of Mb in the absence (curve a) and presence of different amounts of Brij 56 (from curve b to curve d) were presented in Figure 1.

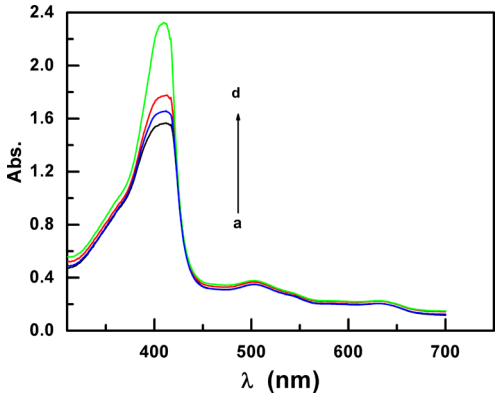

Figure 1. UV−vis spectra of Mb in the absence (a) and presence of different amounts of Brij 56 (b−d) in phosphate buffer solution (0.05 M, pH 7.0). Solution contains 0.15 mg/mL Mb and 0, 1 μL, 2 and 10 μL Brij 56 (from b to d), respectively.

Typical Soret band, Q-band, and CT1 band for a high-spin heme with six-coordination were observed in the spectrum of Mb (curve a) at 411, 504, 535, and 634 nm, respectively. These bands also proved that the fifth and sixth coordination position of the iron atom of Mb was bound by a histidine residue (His-93) and a water molecule.[29] The presence of Brij 56 in Mb solution caused little change of the wavelengths and bandwidths of the Soret and Q-bands of Mb (from curve b to d). It was proposed that Mb retained its secondary structure with heme in a high-spin state in the presence of Brij 56. However, the Soret band intensity of Mb increased with the increase of Brij 56 concentrations. An intense Soret band indicated the covalent binding of water to a six-coordinate high-spin ferric heme iron and a distal pocket with high polarity.[30] The presence of Brij 56 made the active site of Mb bind water strongly to preserve the high−spin MbFe(III)−H_2O form.

Circular dichroism (CD) spectroscopy is an important tool to study the secondary structure of proteins. Figure 2 was the CD spectra of Mb without (a) and with Brij 56 (b). The two peaks at 208 and 222 nm indicated the presence of α-helical portions in Mb.[31] In the presence of Brij 56 (curve b), almost no changes were observed in the CD spectrum of Mb, indicating that Mb retained its second structure in Brij 56 matrix.

The interaction between Mb and Brij 56 can also be characterized by FT-IR spectroscopy. Figure 3 showed the spectra of Brij 56 (a), Mb (b), and Mb-Brij 56 composite (c). The broad band of Figure 3a at 3353−3500 cm^{-1} corresponded to the hydroxyl groups, and the band at 2960−2970 cm^{-1} corresponded to the C−H stretch of Brij 56. For Mb (Figure 3, curve b), the adsorption band at 1538 cm^{-1} was caused by bending and stretching of the N−H and C−N bond, which belongs to amide II group. The band at 1660 cm^{-1} could be assigned to C═O stretching of α-helical conformation (amide I).[32] Of the different bands originating from the peptide linkage, only the amide I band has been proved to contain significant information about the secondary structure of

DOI: 10.1021/acsami.5b01492
ACS Appl. Mater. Interfaces 2015, 7, 11286−11293

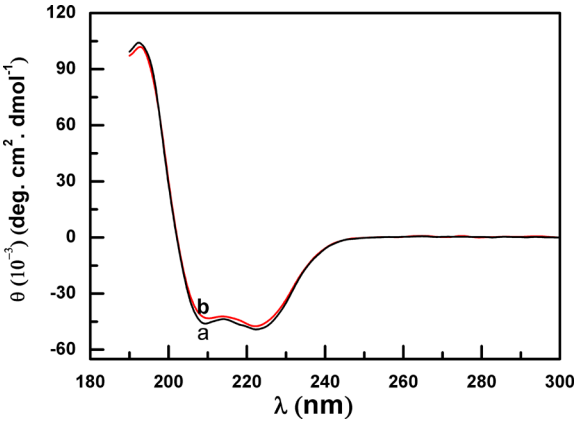

Figure 2. CD spectra of Mb (a) and MB-Brij 56 (b) in phosphate buffer solution (0.05 M, pH 7.0). Solution contains 0.15 mg/mL Mb and 10 μL Brij 56.

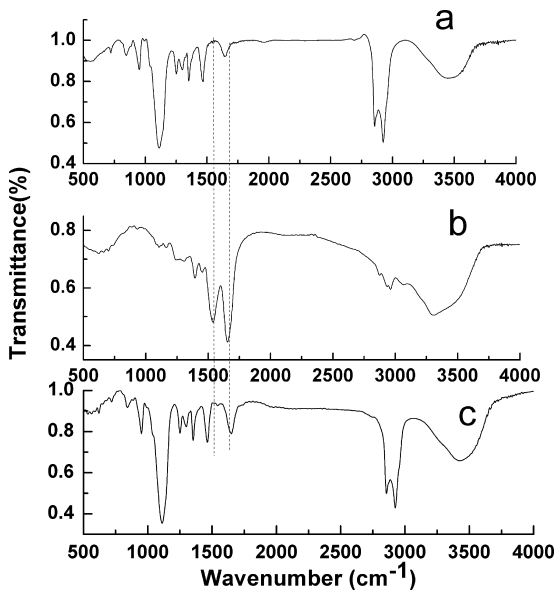

Figure 3. FT-TR spectra of Brij 56 (a), Mb (b), and Mb-Brij 56 (c).

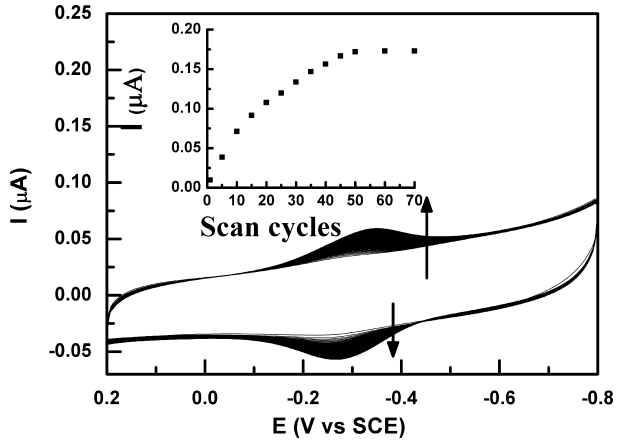

Figure 4. Consecutive CVs of the Brij 56/GCE in 0.05 M phosphate buffer (pH 7.0) with 4 mg/mL Mb. Scan rate: 50 mV/s. (inset) Relationship between the scan cycle numbers and the currents of the anodic peak.

4. Steady peak current was achieved after ca. 50 cycles, indicating the saturation of Mb in the Brij 56 film.

Scheme 1 illustrated the assembly and DET of Mb at the Brij 56-modified GCE. Brij 56 is a nonionic surfactant with a long

Scheme 1. Illustration of the Assembly and DET of Mb on Brij 56/GCE

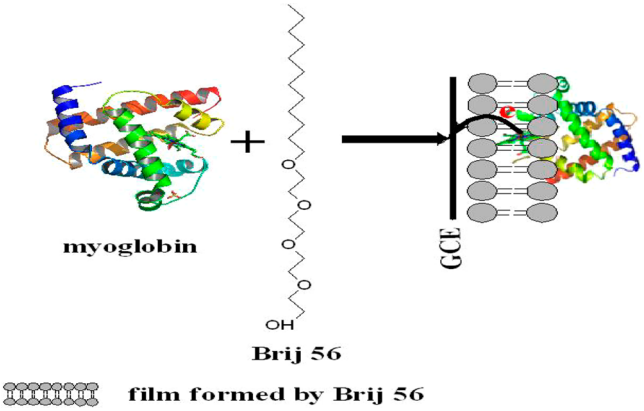

proteins.[33] Almost no change was observed in the amide I region for Mb-Brij 56 mixture (curve c), indicating that Mb preserved its secondary structure in the presence of Brij 56. The amide II band position can be analyzed to get the information about the environment and hydrogen-bonding characteristics of the peptide NH bonds.[34] The amide II band shifted to higher wavenumbers by ~80 cm^{-1}, indicating the formation of hydrogen bonds between Mb and Brij 56.[35]

3.2. Immobilization and Orientation of Mb in the Brij 56 Modified Electrode. Cyclic voltammetric method has been used to immobilize Mb in Brij 56 modified electrode. The continuous CV responses of 4 mg/mL Mb in 0.05 M phosphate buffer solution (pH 7.0) at the Brij 56 modified GCE was displaced in Figure 4. A pair of very tiny redox peaks appeared during the first scan cycle. When the scan numbers increased, the cathodic and anodic peak currents increased too. The formal potential (E_0') of this redox pair is −310 mV (vs SCE). It coincides well with the voltammetric signal of heme Fe(III)/Fe(II) of Mb.[36] The relationship between anodic peak currents (I_{pa}) and scan cycles was shown in the inset of Figure

hydrocarbon tail. It would self-assemble into a uniform bilayer on the GCE surface. Mb is a hemoprotein with spherical shape. It comprises of a single polypeptide chain and a heme active site. It would enter into the film because of the hydrophobic interaction between Mb and Brij 56. When a small electric field was applied, some defects were formed on the Brij 56 biomembrane due to the phase transition of the surfactant layers from solid to liquid phases during electrochemical experiment.[37,38] Mb went through the fluid Brij 56 bilayer during the CV cycling process. The in situ reconstruction of the Brij 56 bilayer around the entrapped Mb was benefit for the favorable orientation of Mb, and thus DET of the entrapped Mb was realized. The characterizations of the interaction between Brij 56 and Mb confirmed that the tertiary structure of Mb insert into the Brij 56 membrane changed, while its secondary structure was kept. The microenvironment Brij 56 provided is the same as that of Mb in native statuses, and the phase transitions of Brij 56 during CV process gave Mb more freedom in orientation. Since reorientation of the protein was essential for a quick electron transfer,[39] the favorable

DOI: 10.1021/acsami.5b01492
ACS Appl. Mater. Interfaces 2015, 7, 11286−11293

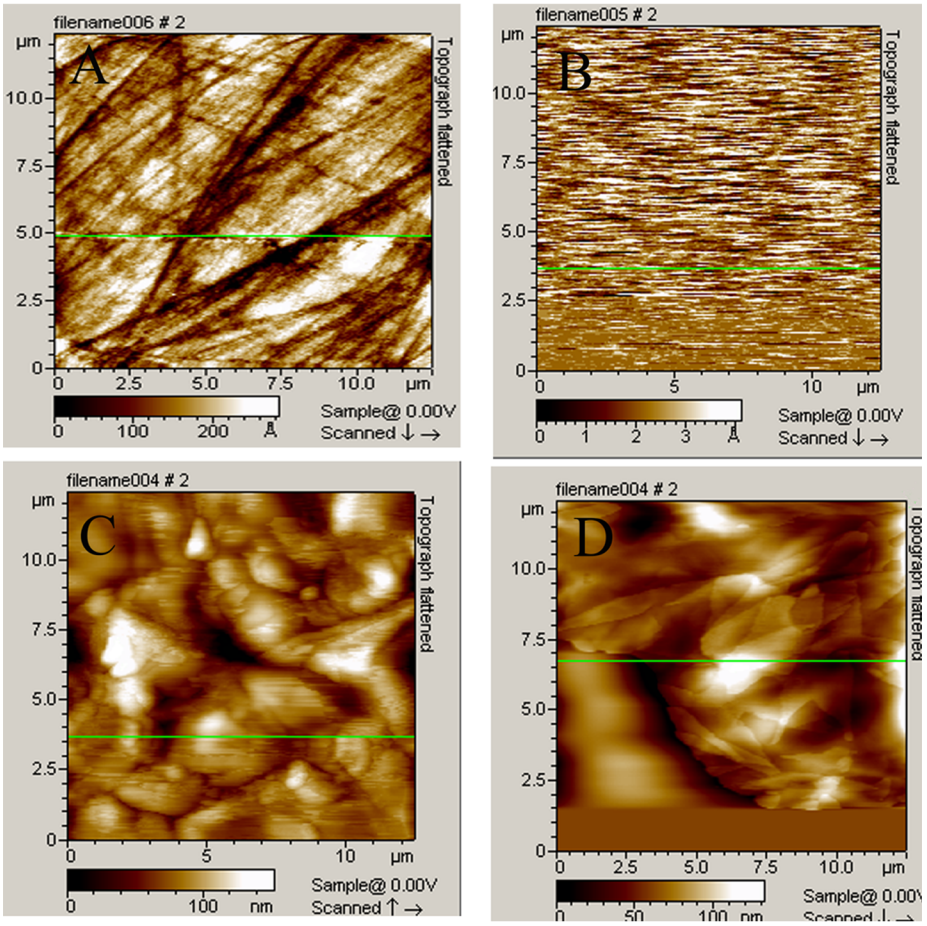

Figure 5. Tapping-mode AFM topographic images of freshly polished GCE (A), Brij 56/GCE (B), Mb-Brij 56/GCE (C), and Mb/Brij 56/GCE (D).

orientation of Mb in Brij 56 film increased the exposure of the active site of proteins and facilitated the electron transfer. Hydrogen-bonding networks formed between Brij 56 and lysine ($-NH_3^+$) groups around the active site of Mb also are very important for DET.[40] Good orientation of Mb into the Brij 56 film due to these hydrogen bonds allowed the rapid electron transfer between the electrode surface and the active site of Mb.

The immobilization and orientation of Mb in the Brij 56-modified electrode was also studied by AFM measurements. Figure 5A showed that the surface of the bare GCE was homogeneous. The lines on the surface were caused by the mechanical alumina polishing. An almost featureless surface after the modification of GCE by Brij 56 was observed (Figure 5 B). The immobilization of Mb in the Brij 56 film by CV method made the membrane surface rough, as showed in Figure 5C. The globular Mb was deposited over the surface homogeneously and densely. However, irregular coverage and higher agglomeration was observed on the Mb/Brij56/GCE surface (Figure 5D). Therefore, it seemed that the CV method is efficient for the immobilization and orientation of Mb in Brij 56 film.

3.3. Direct Electrochemical Characters of Mb Immobilized into Brij 56 Film. The direct electrochemistry of Mb immobilized into Brij 56 film was studied by CVs. Figure 6 depicted CVs of unmodified, Brij 56, Mb/Brij 56, and Mb-Brij56-modified electrodes in N_2-saturated 0.05 M phosphate buffer solution (pH 7.0) when the applied scan rate was 100

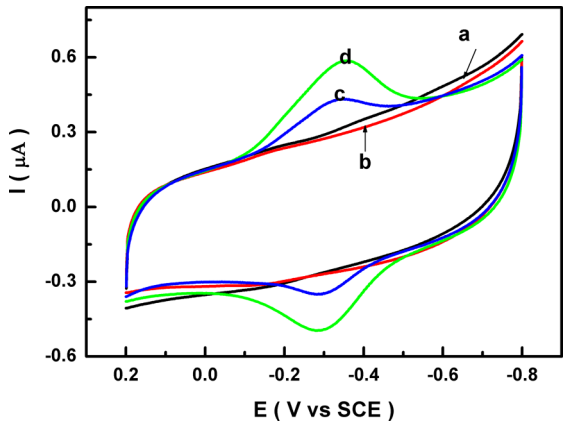

Figure 6. CVs of unmodified (a), Brij56 (b), Mb and Brij56-modified GCE by casting the mixture of Brij 56 and Mb (c) and Mb-Brij56/GCE (d) modified by CV method in 0.05 M phosphate buffer (pH 7.0) at the scan rate of 100 mV/s.

mV s^{-1}. The redox peak did not appear at the unmodified (curve a) and Brij 56-modified GCE (curve b), indicating that no electrochemical reaction occurred in the investigated potential range. For Mb/Brij 56/GCE and Mb-Brij 56/GCE, both of them (curve c and d) have the characters of a pair of stable peaks for Mb−Fe(III)/Fe(II) redox couple at −289 and −339 mV (vs SCE). The observed quasi-reversible redox peaks were attributed to the well-known reaction of heme-Fe^{3+} + e^-

DOI: 10.1021/acsami.5b01492
ACS Appl. Mater. Interfaces 2015, 7, 11286−11293

→ heme-Fe^{2+}. This suggested that Brij 56 could act as a promoter to assist the direct electron transfer of Mb. However, the peak current of Mb-Brij 56/GCE (curve d) was larger than that of Mb/Brij 56/GCE (curve c). It might be due to the well orientation of Mb in the Brij 56 film when it was assembled on the electrode by the electrochemical method. The electron tunneling distance between Mb and the underlying electrode was decreased by the hydrogen bond. Thus, the electron transfer rates were enhanced and eventually amplified the DET signal of Mb. Mb at Brij 56/GCE displayed characteristics of quasi-reversible behavior. For the DET process, the potential separation of the forward and reverse peaks (ΔEp = Epa − Epc) was ∼59 mV when the scan rate was 100 mV/s, and the peak current ratio (Ipa/Ipc) was ∼0.99.[41] The small ΔEp value indicated that the DET of the Mb−Fe^{3+}/Fe^{2+} redox couple in the Brij 56 matrix was fast.

The characteristics of Mb oriented in Brij 56 film were further investigated by studying the scan rates on the peak currents of the immobilized Mb. Figure 7 presented the CVs of

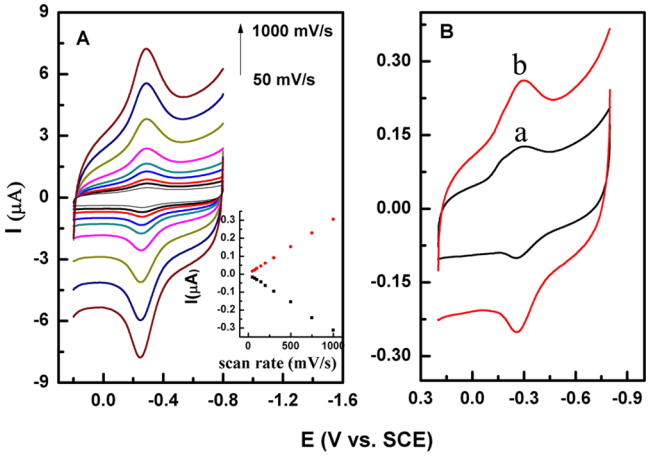

Figure 7. (A) CVs of Mb-Brij56/GCE at different scan rates (50−1000 mV/s). (inset) The relationship between the scan rates and peak currents in 0.05 M phosphate buffer (pH 7.0). (B) CVs of Mb-Brij56/GCE in 0.05 M phosphate buffer (pH7.0) at low scan rates of 10(a) and 25 (b) mV/s.

Mb-Brij 56/GCE obtained at different scan rates in phosphate buffer solution (pH 7.0). The heights of the anodic and cathodic peak currents of the redox pairs were nearly equal at each scan rate. When the scan rate was below or equal to 10 mV/s, Mb Fe(II) was autooxidized by the residual oxygen in the phosphate solution and thus caused a new peak at the left of the reduction peak (curve a in Figure 7B). When the scan rate was 50 mV/s or above, symmetric CVs were obtained because the oxidation of Mb Fe(II) was mainly electrochemically driven, while the autoxoidation of Mb Fe(II) was negligible (curve b in Figure 7B). The linear relationships between the scan rates and redox peak currents were obtained. For the cathodic peaks, the linear regression equation was I_{pa} (μA) = 10.67υ (V s^{-1}) + 0.042 (r = 0.998). For the anodic peaks, the linear regression equation was I_{pc} (μA) = −10.58υ (V s^{-1}) − 0.058 (r = 0.998) (Figure 7B). The cathodic and anodic peak positions remained unchanged when the scan rates were less than 1000 mV/s. These electrochemical characteristics indicated a surface-controlled reaction process for the immobilized Mb. The CVs of the immobilized Mb kept stable after consecutive potential cycling, indicating that Brij 56 was biocompatible for the stable orientation of Mb. The constant charge (Q) values obtained at different scan rates by integrating the reduction peaks were equal. The surface concentration (Γ) of the immobilized electroactive Mb was ∼3.84 × 10^{-11} mol/cm^2 be estimated by Faraday's Law.[42] This value was close to the theoretical monolayer coverage (about 2.0 × 10^{-11} mol/cm^2),[43] suggesting that one layer Mb was immobilized on Brij 56. These electroactive Mb could transfer electrons from its active site to the underlying electrode in the phosphate buffer thus contributed to the observed redox peaks.

The average electron transfer rate constant (k_s) for Mb immobilized in Brij 56 film was estimated to be 72.6 ± 3 s^{-1} by using the Laviron's method.[44] This k_s value was higher than that observed for Mb immobilized on nanoplated lanthanum-substituted bismuth titanate microspheres (10.4 s^{-1})[43] and Mb on silver nanoparticles (3.02 s^{-1}).[45] This implied that the electron transfer from the active sites of the immobilized Mb to the underlying electrode was facilitated by Brij 56. Possible reasons for the faster electron transfer of Mb in Brij 56 film include: (1) The favorable orientation of Mb immobilized in the film by CV method was of benefit to the electron exchange between Mb and electrode; and (2) Macromolecular impurities from solutions would be adsorbed on bare GCEs and block the electron transfer of Mb,[46] but this adsorption was prevented after the electrode was covered by Brij 56.

The solution pH has a significant influence on the direct electrochemistry characters of Mb immobilized in Brij 56 film, as is shown in Figure 8. The anodic and cathodic peaks of the

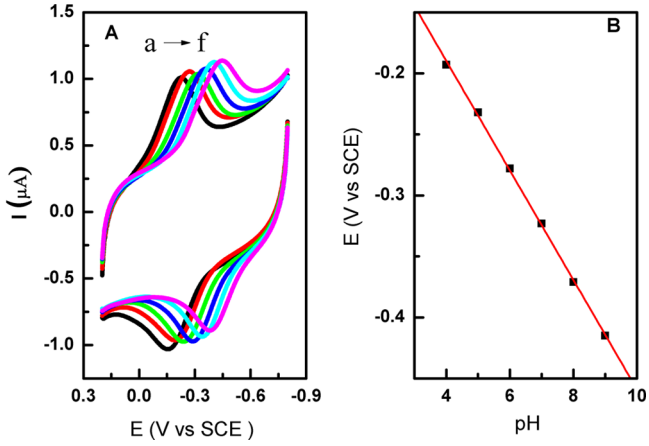

Figure 8. (A) CVs of Mb-Brij56/GCE in 0.05 M phosphate buffer at different pH (from a to f: 4.0−9.0) and (B) linear relationship between pH and formal potentials at a scan rate of 100 mV/s.

immobilized Mb were well-defined in all the studied pH ranges. However, the negative shift of both of the peaks was observed when the pH was increased from 4.0 to 9.0, indicating the participation of protons in the electrochemical process. The linear relationship between pH and the formal potential indicated that the electron transfer of the immobilized Mb was a proton transfer coupled electron transfer process.[47] Compared with the theoretical value of 59 mV/pH for equal proton-coupled electron transfer process,[48] the slope of −44.91 mV/pH of this system was a little bit smaller. It may be due to the protonation of the coordinated water molecule around Mb Fe(II).

3.4. Electrocatalytic Response of Nitrite at Mb-Brij 56/GCE. Nitrite has been widely used to preserve food products,

DOI: 10.1021/acsami.5b01492
ACS Appl. Mater. Interfaces 2015, 7, 11286−11293

but it always is associated with the formation of carcinogens.[49] The electrochemical reduction of nitrite on the Mb-modified electrodes[49−51] has been used for nitrite detection with relatively good selectivity, high sensitivity, fast response, and without separation. Figure 9A showed the CVs of the Brij56-Mb/GCE in phosphate buffer solution with different concentrations of nitrite. The presence of nitrite in the solution caused the appearance of a new catalytic reduction peak at ca. −780 mV. The increasing of the concentration of nitrite (from curve c to curve f in Figure 9A) was accompanied by the increase of the currents of this peak. Similar results have been found by Farmer et al. with the Mb-didodecyldimethylammonium bromide (DDAB) modified pyrolytic graphite electrode[50] and Ju et al. with Mb immobilized on a kind of silica with hexagonal mesoporous structure.[52] However, this redox peak did not appear at the Brij 56/GCE under the same conditions without Mb (curves a and b in Figure 9A). The results indicated that Mb presented in Brij 56 film exhibited excellent catalytic performance to the reduction of nitrite. The pathway suggested by Farmer et al.[50] could be used to elucidate the catalytic reduction mechanism of nitrite on the Brij 56-Mb/GCE. NO produced from the nitrite disproportionation reaction was catalytically reduced by Mb-Brij 56 and thus caused the enhancement of the peak currents at −780 mV. Figure 9B displayed the dependence of the amperometric response of the Mb-Brij 56/GCE on the concentration of $NaNO_2$ at an applied potential of −800 mV (vs SCE). $NaNO_2$ was reduced quickly at the Mb-Brij 56/GCE with a steeply increased peak current, and the currents were proportional to the concentration of $NaNO_2$. A calibration curve was established to describe the relationship between the concentrations of $NaNO_2$ and the peak currents (inset of Figure 9). The linear response range of the sensor to NO_2^- concentration was from 10.0 to 292 μM (R^2 = 0.9997). The detection limit of this biosensor was 4.8 μM (S/N = 3), below the reported detection limit of 0.01 mM.[53]

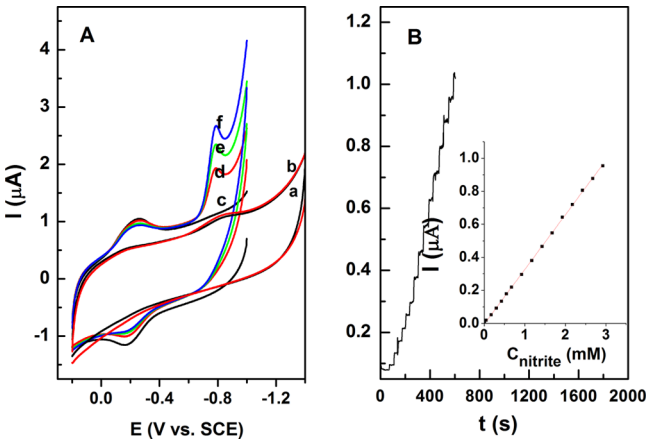

Figure 9. (A) CVs at 0.1 V s^{-1} in 10.0 mL of phosphate buffer (pH 5.5) for Brij56/GCE (a), Mb-Brij56/GCE in buffers without $NaNO_2$ (c), (b) Brij56/GCE in buffers containing 1.5 mM $NaNO_2$, and Mb-Brij 56/GCE containing different concentrations of $NaNO_2$ (from d to f): 0.5, 1.0, and 1.5 mM. (B) Amperometric responses recorded at the Mb-Brij 56/GCE in a stirred solution during the additions of different concentrations of $NaNO_2$. (inset) The calibration plot for nitrite obtained with the Mb-Brij 56/GCE. Background electrolyte, 0.05 M phosphate buffer solution (pH 5.5), applied potential, −800 mV.

The CV peak potentials and currents of Mb-Brij56/GCE were checked to study the stability of the biosensor. When the biosensor was kept in a refrigerator for 30 d, the CV peak potentials of the redox peaks of Mb changed a little, and the peak currents retained 92.5% of the initial value. The biosensor was also used to detect the same concentrations of $NaNO_2$ each day. For 20.0 μM NO_2^-, the biosensor maintained 91.3% of its initial activity after a month. Thus, Brij 56 supplied a suitable microenvironment to keep the enzyme activity of Mb.

4. CONCLUSIONS

This work verified that Brij 56 could be used as an appropriate matrix to stabilize the catalytic intermediates of proteins. Electrochemical method has been proved to assist the immobilization and orientation of Mb in the Brij 56 film modified electrode. Through oriented immobilization, Mb can be predisposed in a manner that is optimal for binding to its respective ligands and undergoes fast interfacial electron exchange. The method was easy, controllable, and reproducible. The apparent heterogeneous electron transfer rate constant of Mb in Brij 56 film was ~72.6 ± 3 s^{-1}. Electrocatalysis of the immobilized Mb toward nitrite shows that this method can be expanded to other protein to fabricate novel biosensors.

AUTHOR INFORMATION

Corresponding Authors

*E-mail: yz_xiner@163.com. (Q.X.)
*E-mail: xyhu@yzu.edu.cn. (X.-Y.H.)

Author Contributions

The manuscript was written through contributions of all authors. All authors have given approval to the final version of the manuscript.

Notes

The authors declare no competing financial interest.

ACKNOWLEDGMENTS

The authors gratefully acknowledge NSFC (21275124 and 21275125), the Foundation of Jiangsu Educational Bureau (12KJB150022) and Yangzhou Environmental Protection Bureau (YHK1410), the Qinglan Project of JiangSu Province (11KJB150019), Open Project of State Key Laboratory of Analytical Chemistry for Life Science (SKLACLS1414), the high-end talent project of Yangzhou University, and the project funded by the PAPD.

REFERENCES

(1) Peng, H.; Liang, R.; Qiu, J. Facile Synthesis of Fe_3O_4@Al_2O_3 Core-Shell Nanoparticles and their Application to the Highly Specific Capture of Heme Proteins for Direct Electrochemistry. *Biosens. Bioelectron.* **2011**, *26*, 3005−3011.
(2) Mao, S.; Long, Y.; Li, W.; Tu, Y.; Deng, A. Core-Shell Structured Ag@C for Direct Electrochemistry and Hydrogen Peroxide Biosensor Applications. *Biosens. Bioelectron.* **2013**, *48*, 258−262.
(3) Leech, D.; Kavanagh, P.; Schuhmann, W. Enzymatic Fuel Cells: Recent Progress. *Electrochim. Acta* **2012**, *84*, 223−234.
(4) Cheng, H.; Qian, Q.; Wang, X.; Yu, P.; Mao, L. Electricity Generation from Carboxymethyl Cellulose Biomass: a New Application of Enzymatic Biofuel Cells. *Electrochim. Acta* **2012**, *82*, 203−207.
(5) Vincent, K. A.; Li, X.; Blanford, C. F.; Belsey, N. A.; Weiner, J. H.; Armstrong, F. A. Enzymatic Catalysis on Conducting Graphite Particles. *Nat. Chem. Biol.* **2007**, *3*, 761−762.
(6) Tian, Y.; Mao, L.; Okajima, T.; Ohsaka, T. Electrochemistry and Electrocatalytic Activities of Superoxide Dismutases at Gold Electrodes

DOI: 10.1021/acsami.5b01492
ACS Appl. Mater. Interfaces 2015, 7, 11286−11293

Modified with a Self-Assembled Monolayer. *Anal. Chem.* **2004**, *76*, 4162−4168.
(7) Chaplin, M. F.; Bucke, C. *Enzyme Technology;* Cambridge University Press: Cambridge, U.K., 1990.
(8) Pita, M.; Katz, E. Multiple Logic Gates Based on Electrically Wired Surface-Reconstituted Enzymes. *J. Am. Chem. Soc.* **2008**, *130*, 36−37.
(9) Heller, A. Electrical Wiring of Redox Enzymes. *Acc. Chem. Res.* **1990**, *23*, 128−134.
(10) Rüdiger, O.; Abad, J. M.; Hatchikian, E. C.; Fernandez, V. M.; DeLacey, A. L. Oriented Immobilization of Desulfovibrio Gigas Hydrogenase onto Carbon Electrodes by Covalent Bonds for Nonmediated Oxidation of H_2. *J. Am. Chem. Soc.* **2005**, *127*, 16008−16009.
(11) Sethuraman, A.; Belfort, G. Protein Structural Perturbation and Aggregation on Homogeneous Surfaces. *Biophys. J.* **2000**, *88*, 1322−1333.
(12) Kunitake, T.; Shimomura, M.; Kajiyama, T.; Harada, A.; Okuyama, K.; Takayanagi, M. Ordered Cast Films of an Azobenzene-containing Molecular Membrane. *Thin Solid Films* **1984**, *121*, L89−L91.
(13) Rusling, J. F.; Zhang, Z. Biomolecules, Biointerface, and Applications. In *Handbook of Surfaces and Interfaces of Materials;* Nalwa, H. S., Ed.; Academic Press: San Diego, CA, 2001; Vol. *5*, pp 33−71.
(14) Xu, Y. X.; Hu, C. G.; Hu, S. S. Single-Chain Surfactant Monolayer on Carbon Paste Electrode and its Application for the Studies on the Direct Electron Transfer of Hemoglobin. *Bioelectrochemistry* **2009**, *74*, 254−259.
(15) Ma, W.; Ying, Y.-L.; Qin, L.-X.; Gu, Z.; Zhou, H.; Li, D.-W.; Sutherland, T. C.; Chen, H.-Y.; Long, Y.-T. Investigating Electron-Transfer Processes Using a Biomimetic Hybrid Bilayer Membrane System. *Nat. Protoc.* **2013**, *8*, 439−450.
(16) Rusling, J. F.; Nassar, A.-E. F. Enhanced Electron Transfer for Myoglobin in Surfactant Films on Electrodes. *J. Am. Chem. Soc.* **1993**, *115*, 11891−11897.
(17) Chen, X. L.; Hu, N. F.; Zeng, Y. H.; Rusling, J. F.; Yang, J. Ordered Electrochemically Active Films of Hemoglobin, Didodecyldimethylammonium Ions, and Clay. *Langmuir* **1999**, *15*, 7022−7030.
(18) Lu, Q.; Hu, C. G.; Cui, R.; Hu, S. S. Direct Electron Transfer of Hemoglobin Found on Electron Tunneling of CTAB Monolayer. *J. Phys. Chem. B* **2007**, *111*, 9808−9813.
(19) Das, T. K.; Mazumdar, S.; Mitra, S. Micelle Induced Release of Heme NO from Nitric Oxide Complex of Myoglobin. *J. Chem. Soc., Chem. Commun.* **1993**, 1447−1448.
(20) Das, T. K.; Mazumdar, S. pH Induced Conformational Perturbation of Horseradish Peroxidase -Pico Second Tryptophan Fluorescence Studies on Native and Cyanide Modified Enzymes. *Biochim. Biophys. Acta* **1994**, *1209*, 227−237.
(21) Chen, S.; Tseng, C. Comparison of the Direct Electrochemistry of Myoglobin and Hemoglobin Films and their Bioelectrocatalytic Properties. *J. Electroanal. Chem.* **2005**, *575*, 147−160.
(22) Huang, Q. D.; Lu, Z. Q.; Rusling, J. F. Composite Films of Surfactants, Nafion, and Proteins with Electrochemical and Enzyme Activity. *Langmuir* **1996**, *12*, 5472−5480.
(23) Zhao, D. D.; Zhou, W. J.; Li, H. L. Effects of Deposition Potential and Anneal Temperature on the Hexagonal Nanoporous Nickel Hydroxide Films. *Chem. Mater.* **2007**, *19*, 3882−3891.
(24) Chen, Z.; Jiang, Y. B.; Dunphy, D. R.; Adams, D. P.; Hodges, C.; Liu, N. G.; Zhang, N.; Xomeritakis, G.; Z.Jin, X.; Aluru, N. R.; Gaik, S. J.; Hillhouse, H. W.; Brinker, C. J. DNA Translocation through an Array of Kinked Nanopores. *Nat. Mater.* **2010**, *9*, 667−675.
(25) Zhao, D.; Huo, Q.; Jianglin, F.; Chmelka, B. F.; Stucky, G. D. Nonionic Triblock and Star Diblock Copolymer and Oligomeric Surfactant Syntheses of Highly Ordered, Hydrothermally Stable, Mesoporous Silica Structures. *J. Am. Chem. Soc.* **1998**, *120*, 6024−6036.
(26) Kang, Z.; Yan, X. Q.; Zhang, Y.; Shi, J.; Zhang, X. H.; Liu, Y.; Choi, J. H.; Porterfield, D. M. Single-Stranded DNA Functionalized Single-Walled Carbon Nanotubes for Microbiosensors via Layer-by-Layer Electrostatic Self-Assembly. *ACS Appl. Mater. Interfaces* **2014**, *6*, 3784−3789.
(27) Weidinger, I. M.; Murgida, D. H.; Dong, W.-f.; Mohwald, H.; Hildebrandt, P. Redox Processes of Cytochrome C Immobilized on Solid Supported Polyelectrolyte Multilayers. *J. Phys. Chem. B* **2006**, *2006*, 522−529.
(28) Munge, B.; Estavillo, C.; Schenkman, J. B.; Rusling, J. F. Optimization of Electrochemical and Peroxide-Driven Oxidation of Styrene With Ultrathin Polyion Films Containing Cytochrome P450cam And Myoglobin. *ChemBioChem* **2003**, *4*, 82−89.
(29) Eaton, W. A.; Hochstrasser, R. M. Single-Crystal Spectra of Ferrimyoglobin Complexes in Polarized Light. *J. Chem. Phys.* **1968**, *49*, 985−995.
(30) Ikeda-Saito, M.; Hori, H.; Andersson, L.; Prince, R.; Pickering, I.; Goerge, G.; Saunders, C.; Lutz, R.; Mckelvey, E.; Maltera, R. Coordination Structure of the Ferric Heme Iron in Engineered Distal Histidine Myoglobin Mutants. *J. Biol. Chem.* **1992**, *267*, 22843−22852.
(31) Woody, R. W. *Circular Dichroism: Principles and Applications;* VHC Publishers: New York, 1994; p 473.
(32) Adams, S.; Higgins, A. M.; Jones, R. A. L. Heme Protein-Clay Films: Direct Electrochemistry and Electrochemical Catalysis. *Langmuir* **2002**, *18*, 4854−4861.
(33) Krimm, S.; Bandekar, J. Vibrational Spectroscopy and Conformation of Peptides, Polypeptides, and Proteins. *Adv. Protein Chem.* **1986**, *38*, 181−364.
(34) Myshakina, N. S.; Ahmed, Z.; Asher, S. A. Dependence of Amide Vibrations on Hydrogen Bonding. *J. Phys. Chem. B* **2008**, *112*, 11873−11877.
(35) Gray, J. L.; Barnes, C. M.; Carr, A. J.; McCAIN, K. S. Effect of Hydrogen Bonding on the Amide II Band of Model Disubstituted Urea Compounds. *Appl. Spectrosc.* **2009**, *63*, 1409−1413.
(36) Ray, A.; Feng, M.; Tachikawa, H. Direct Electrochemistry and Raman Spectroscopy of Sol-Gel-Encapsulated Myoglobin. *Langmuir* **2005**, *21*, 7456−7460.
(37) Nassar, A. E. F.; Willis, W. S.; Rusling, J. F. Electron transfer from Electrodes to Myoglobin: Facilitated in Surfactant Films and Blocked by Adsorbed Biomacromolecules. *Anal. Chem.* **1995**, *67*, 2386−2392.
(38) Kotyk, A.; Janacek, K.; Koryta, J. *Biophysical Chemistry of Membrane Function;* John Wiley & Sons: New York, 1988; p 41−115.
(39) Jin, B.; Wang, G.-X.; Millo, D.; Hidebrandt, P.; Xia, X.-H. Electric-field Control of the pH-Dependent Redox Process of Cytochrome C Immobilized on a Gold Electrode. *J. Phys. Chem. C* **2012**, *116*, 13038−13044.
(40) Li, N.; Xu, J. Z.; Yao, H.; Zhu, J. J.; Chen, H. Y. The Direct Electron Transfer of Myoglobin Based on the Electron Tunneling in Proteins. *J. Phys. Chem. B* **2006**, *110*, 11561−11565.
(41) Bard, A. J.; Faulkner, L. R. *Electrochemical Methods;* John Wiley & Sons: New York, 2001.
(42) He, X. Y.; Zhou, L.; Nesterenko, E. P.; Nesterenko, P. N.; Paull, B.; Omamogho, J. O.; Glennon, J. D.; Luong, J. H. T. Porous Graphitized Carbon Monolith as an Electrode Material for Probing Direct Bioelectrochemistry and Selective Detection of Hydrogen Peroxide. *Anal. Chem.* **2012**, *84*, 2351−2357.
(43) Hu, J.; Yu, Y.; Guo, H.; Chen, Z.; Li, A.; Feng, X.; Xi, B.; Hu, G. Sol-gel Hydrothermal Synthesis and Enhanced Biosensing Properties of Nanoplated Lanthanum-Substituted Bismuth Titanate Microspheres. *J. Mater. Chem.* **2011**, *21*, 5352−5359.
(44) Laviron, E. General Expression of the Linear Potential Sweep Voltammogram in the Case of Diffusionless Electrochemical Systems. *J. Electroanal. Chem.* **1979**, *101*, 19−28.
(45) Palanisamy, S.; Karuppiah, C.; Chen, S.-M.; Emmanuel, R.; Muthukrishnan, P.; Prakash, P. Single-Stranded DNA Functionalized Single-Walled Carbon Nanotubes for Microbiosensors via Layer-by-Layer Electrostatic Self-Assembly. *Sens. Actuators, B* **2014**, *202*, 177−184.
(46) King, B. C.; Hawkridge, F. M.; Hoffman, B. M. Electrochemical Studies of Cyanometmyoglobin and Metmyoglobin: Implications for

DOI: 10.1021/acsami.5b01492
ACS Appl. Mater. Interfaces 2015, 7, 11286−11293

Long-Range Electron Transfer in Proteins. *J. Am. Chem. Soc.* **1992**, *114*, 10603−10608.
(47) Liu, H.; Tian, Z.; Lu, Z.; Zhang, Z.; Zhang, M.; Pang, D. Direct Electrochemistry and Electrocatalysis of Heme-Proteins Entrapped in Agarose Hydrogel Films. *Biosens. Bioelectron.* **2004**, *20*, 294−304.
(48) Zhou, Y.; Hu, N.; Zeng, Y.; Rusling, J. Heme protein-clay films: direct electrochemistry and electrochemical catalysis. *Langmuir* **2002**, *18*, 211−219.
(49) Liu, S.; Ju, H. Nitrite Reduction and Detection at a Carbon Paste Electrode Containing Hemoglobin and Colloidal Gold. *Analyst* **2003**, *128* (12), 1420−1424.
(50) Lin, R.; Bayachou, M.; Greaves, J.; Farmer, P. J. Nitrite Reduction by Myoglobin in Surfactant Films. *J. Am. Chem. Soc.* **1997**, *119*, 12689−12690.
(51) Xu, M. Q.; Wu, J. F.; Zhao, G. C. An Amperometric Hydrogen Peroxide Biosensor Based on Myoglobin Immobilized on SDS-GNPs-GR Modified Electrode. *Int. J. Electrochem. Sci.* **2013**, *8*, 6502−6512.
(52) Dai, Z. H.; Xu, X. M.; Ju, H. X. Direct Electrochemistry and Electrocatalysis of Myoglobin Immobilized on a Hexagonal Mesoporous Silica Matrix. *Anal. Biochem.* **2004**, *332*, 23−31.
(53) Yue, R.; Lu, Q.; Zhou, Y. K. A Novel Nitrite Biosensor Based on Single-Layer Graphene Nanoplatelet-Protein Composite Film. *Biosens. Bioelectron.* **2011**, *26*, 4436−4441.

DOI: 10.1021/acsami.5b01492
ACS Appl. Mater. Interfaces 2015, 7, 11286−11293